G3 Genes | Genomes | Genetics

INVESTIGATION

MicroRNA Tissue Atlas of the Malaria Mosquito *Anopheles gambiae*

Lena Lampe and Elena A. Levashina[1]
Vector Biology Unit, Max Planck Institute for Infection Biology, 10117 Berlin, Germany
ORCID IDs: 0000-0003-2667-7426 (L.L.); 0000-0003-4605-906X (E.A.L.)

ABSTRACT *Anopheles gambiae* mosquitoes transmit the human malaria parasite *Plasmodium falciparum*, which causes the majority of fatal malaria cases worldwide. The hematophagous lifestyle defines mosquito reproductive biology and is exploited by *P. falciparum* for its own sexual reproduction and transmission. The two main phases of the mosquito reproductive cycle, previtellogenic (PV) and postblood meal (PBM), shape its capacity to transmit malaria. Transition between these phases is tightly coordinated to ensure homeostasis between mosquito tissues and successful reproduction. One layer of control is provided by microRNAs (miRNAs), well-known regulators of blood meal digestion and egg development in *Aedes* mosquitoes. Here, we report a global overview of tissue-specific miRNAs (miRNA) expression during the PV and PBM phases and identify miRNAs regulated during PV to PBM transition. The observed coordinated changes in the expression levels of a set of miRNAs in the energy-storing tissues suggest a role in the regulation of blood meal-induced metabolic changes.

KEYWORDS
Anopheles gambiae
Plasmodium falciparum
microRNAs
reproductive cycle

Anopheles gambiae females are major vectors of the human malaria parasite *Plasmodium falciparum* in sub-Saharan Africa. Mosquito females require a blood meal for egg production, which the parasite exploits as a route of transmission and development, thus linking the mosquito infection and its reproductive (also called gonotrophic) cycle. As reproduction is central to every organism, the hematophagic lifestyle directs mosquito behavior, physiology, and metabolism. The gonotrophic cycle is divided into two phases: the PV and PBM phases. During the PV phase, egg maturation (vitellogenesis) is arrested at a premature stage until the blood meal-mediated uptake of amino acids and lipids (Hagedorn *et al.* 1977; Hansen *et al.* 2014; Smykal and Raikhel 2015). The PV phase, maintained by the juvenile hormone (JH), prepares the carbohydrate-consuming female mosquitoes for blood feeding by accumulating energy resources in the fat body, the major storage tissue in insects, and by activating their host-seeking behavior (Shapiro and Hagedorn 1982; Lu *et al.* 2007; Clifton and Noriega 2011; Perez-Hedo *et al.* 2014; Hou *et al.* 2015; Wang *et al.* 2017). Successful blood feeding initiates the PBM phase, which is driven by the steroid hormone ecdysone (Spielman *et al.* 1971; Hagedorn *et al.* 1975). Amino acids, released into the mosquito circulatory system after blood meal digestion, activate the target of rapamycin (TOR) pathway (Hansen *et al.* 2004, 2005; Attardo *et al.* 2005). TOR, together with ecdysone synthesized from the blood-borne cholesterol, triggers expression of lipid transporters such as lipophorin and vitellogenin that deliver lipids to the developing ovaries (Hansen *et al.* 2004, 2014; Park *et al.* 2006; Zhu *et al.* 2006). Within 48 hr, a blood meal is fully digested, nutrients absorbed, and oogenesis is completed. However, a blood meal may also bring *Plasmodium* infective stages or gametocytes that fuse in the mosquito midgut to produce motile ookinetes (Bennink *et al.* 2016). The ookinetes traverse the midgut epithelium at 18–24 hr PBM and establish an infection at the basal side of the midgut wall (Bennink *et al.* 2016). Here, within the next 10 d, the parasites undergo replication and maturation of the infective forms (Beier 1998). Disruption of the gonotrophic cycle by ecdysone analogs or by restriction of lipid trafficking decreases *Plasmodium* development (Atella *et al.* 2009; Rono *et al.* 2010; Childs *et al.* 2016; Costa *et al.* 2017). Therefore, the PBM phase shapes both mosquito reproduction and *P. falciparum* development, two crucial components of malaria transmission. Repeated blood feedings increase female reproductive fitness by boosting its nutritional resources, and promote *P. falciparum* development by providing key nutrients and a route for transmission to the next host.

Copyright © 2018 Lampe, Levashina
doi: https://doi.org/10.1534/g3.117.300170
Manuscript received August 18, 2017; accepted for publication November 7, 2017; published Early Online November 16, 2017.
This is an open-access article distributed under the terms of the Creative Commons Attribution 4.0 International License (http://creativecommons.org/licenses/by/4.0/), which permits unrestricted use, distribution, and reproduction in any medium, provided the original work is properly cited.
Supplemental material is available online at www.g3journal.org/lookup/suppl/doi:10.1534/g3.117.300170/-/DC1.
[1]Corresponding author: Max Planck Institute for Infection Biology, Charitéplatz 1, 10117 Berlin, Germany. E-mail: levashina@mpiib-berlin.mpg.de

The metabolic transition from the PV to PBM phase entails a complex regulatory network of hormonal, transcriptional, and post-transcriptional changes in multiple tissues. However, the mechanisms of tissue homeostasis during this transition remain incompletely understood. Recently, miRNAs have emerged as powerful regulators of developmental and metabolic switches. miRNAs fine-tune JH and ecdysone pulses and, thereby, shape developmental transitions in the fruit flies (Jin *et al.* 2012; Boulan *et al.* 2013; Verma and Cohen 2015). In mosquito adults, miR-8, miR-309, miR-275, miR-1174, and miR-1890 have been implicated in the regulation of PBM (Bryant *et al.* 2010; Liu *et al.* 2014; Lucas *et al.* 2015a,b; Zhang *et al.* 2016b; Fu *et al.* 2017), and miR-305 in parasite development (Dennison *et al.* 2015). However, in *A. gambiae*, functional studies were performed only for 3 out of 180 miRNAs identified by bioinformatics and experimental approaches (Winter *et al.* 2007; Biryukova *et al.* 2014; Castellano *et al.* 2015; Fu *et al.* 2017). The functional diversity of miRNAs is further amplified by the capacity of each miRNA locus to generate two miRNA arms, which differ in their seed sequence and target distinct sets of mRNAs. Several studies observed a bias in arm selection for different species and tissues, suggesting that it might represent an additional layer of miRNA regulation (Chiang *et al.* 2010; Marco *et al.* 2010; Zhou *et al.* 2012; Biryukova *et al.* 2014). In addition, the same miRNA can regulate distinct processes in a tissue-specific manner by binding different targets. For example, the *Drosophila* miR-8 regulates the production of myogenic peptide hormone in the fat body, whereas it controls synapse structure in the brain (Loya *et al.* 2014; Lee *et al.* 2015). So far, all studies on *A. gambiae* miRNAs have focused either on whole mosquitoes or on few selected tissues (Winter *et al.* 2007; Biryukova *et al.* 2014; Liu *et al.* 2014; Castellano *et al.* 2015; Dennison *et al.* 2015; Fu *et al.* 2017). However, a comprehensive overview of tissue-specific miRNA expression would be beneficial for further characterization of miRNA function during the PV to PBM transition.

Here, we report a global overview of miRNA expression in the head, midgut, abdominal carcass (the fat body), and ovaries of *A. gambiae* females during the transition from the PV to PBM phase, and after *P. falciparum* infection. We show that the majority of mosquito miRNAs are tissue-specific, except for a small cluster of ubiquitously expressed miRNAs. Further, we identify four miRNAs whose expression levels are regulated by blood feeding in the fat body, ovaries, and midgut. Our study provides the first comprehensive miRNA tissue atlas of the female *A. gambiae* mosquito during the gonotrophic cycle and identifies miRNAs with potential roles in this critical process.

MATERIALS AND METHODS

Mosquitoes

We used *A. coluzzii* Ngousso (*TEP1*S1*) mosquitoes. Mosquito lines differ in the genotype of *TEP1*, the major mosquito immune marker. The Ngousso line was initially isolated as a mixed population of *TEP1*S1*, **S2*, and **S1/S2* genotypes. To reduce background genetic variation, we decided to work with the *TEP1*S1* homozygous line to avoid potential genetic interferences. Mosquitoes were reared at 30° and 80% humidity with a 12/12 hr day/night cycle, with 30 min-long dawn/dusk periods. All mosquitoes were fed *ad libitum* with 10% sugar solution.

Blood meal and P. falciparum infections

Blood meals and *P. falciparum* infections were performed using membrane feeders (Lensen *et al.* 1996, 1999). To establish gametocyte cultures, *Pf* NF54 asexual cultures (parasitaemia > 2%) were harvested by centrifugation for 5 min at 1500 rpm, washed with fresh red blood cells, and diluted to 1% total parasitaemia in complete gametocyte medium at 4% hematocrit. Gametocyte cultures were incubated at 37° with 3% O_2 and 4% CO_2. Medium was changed daily for 15–16 d on heated plates to reduce temperature drops. On day 14 after establishment, (i) gametocytaemia was checked by Giemsa stain of gametocyte culture smears and (ii) parasite exflagellation rates were estimated by microscopy.

Mosquitoes were fed with either uninfected or *P. falciparum*-infected blood using an artificial feeder system as described in Lensen *et al.* (1996, 1999). The feeding system was prepared by covering the bottom of the midi-feeders with a stretched parafilm. The midi-feeder was then attached to a 37° water bath system, allowing water flow through the feeder. The blood (Haema, Berlin, Germany) was introduced to the feeder and mosquitoes were fed for 15 min. Unfed mosquitoes were removed and only fully engorged females were kept for further analyses.

Sample collection

Microarray and qPCR: Three-day-old virgin females were divided into three groups and fed with: (i) 10% sugar (sugar-fed; PV phase); (ii) human blood (blood-fed; PBM phase); and (iii) *P. falciparum*-infected blood (infected; PBM phase). After feeding, all groups were kept at 26° and 80% humidity. At 18 hr postfeeding (hpb), 15 females per group were dissected on ice and the heads, midguts, ovaries, and abdominal carcasses were pooled according to the tissue. The samples were homogenized in TRIzol using a beat-beater (QIAGEN) at 50 rpm. Homogenized samples were kept at −80° until further usage.

Time course: For miRNA expression kinetics, 15 unfed and 15 blood-fed females were dissected on ice at 20, 24, 28, 32, and 48 hr after blood meal. The heads, midguts, ovaries, and abdominal carcasses were pooled according to the tissue, immediately homogenized in TRIzol, and kept at −80° for RNA isolation.

RNA isolation

Microarray: Total RNA was isolated using the miRNeasy Mini Kit (QIAGEN) according to the manufacturer's recommendations. Briefly, after phase separation by centrifugation, total RNA was purified by silica membrane, eluted with water, and stored at −80°. The total RNA yield was measured with a NanoDropND-1000 Spectrophotometer. The integrity of total RNA was assessed with a 2100 Bioanalyzer and a RNA 6000 Nano LabChip kit (Agilent). Furthermore, the ratio of miRNA/small RNAs from isolated total RNA was monitored by the Agilent Small RNA kit.

qPCR: Total RNA was isolated by TRIzol according to the manufacturer's recommendations. The total RNA yield was measured with a NanoDropND-1000 spectrophotometer.

Microarray analyses

Custom 8-plex 60K mosquito miRNA microarrays (Design Name: Agilent-049943, ID Name: Custom_Mosquito_miRNA, Design Format: IS-62976-8-V2, AMADID 016436) (Agilent) were used for one-color hybridizations. The microarray included miRNAs identified in *Apis mellifera*, *A. gambiae*, *Tribolium castaneum*, *Culex quinquefasciatus*, *Aedes aegypti*, *Bombyx mori*, and *Drosophila melanogaster*. Total RNA (100 ng) was processed with the miRNA Complete Labeling and Hyb Kit (Agilent), according the supplier's recommendations. In brief, samples were dephosphorylated with Calf Intestine Alkaline Phosphatase and labeled with Cy3 in a T4 RNA ligase-mediated

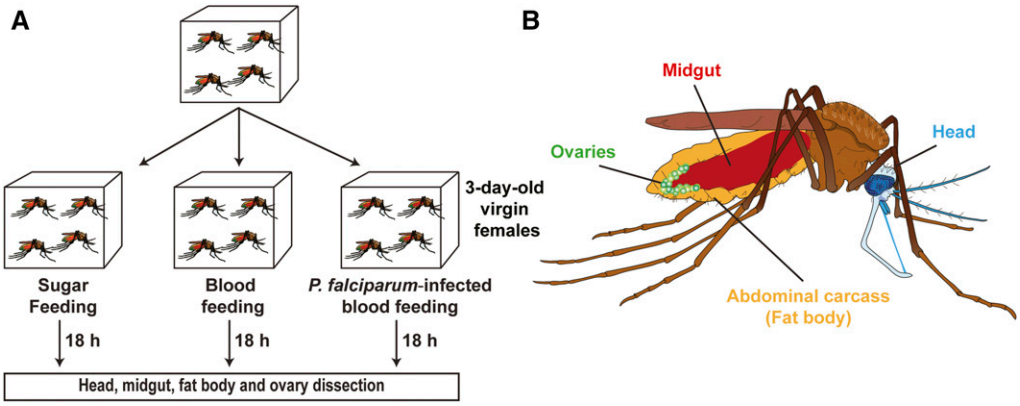

Figure 1 Experimental set up for tissue-specific microRNA (miRNA) expression analysis. (A) Mosquitoes were fed with: (1) 10% sugar, (2) blood, or (3) *P. falciparum*-infected blood. At 18 hr post blood feeding, mosquitoes from each group were dissected. (B) The head, midgut, fat body, and ovaries were examined for tissue-specific miRNA expression.

reaction with 3′,5′-cytidine bisphosphate (Cy3-pCp). The labeling reaction was column-purified, vacuum-dried using a speed-vac at 45°, and resuspended in a blocking and hybridization buffer. After hybridization, the microarrays were washed, scanned at 5 μm resolution with a G2565CA high-resolution laser microarray scanner, and features were extracted. Results were analyzed by the R limma package. Briefly, signal intensities were corrected for the background using the normexp function and quantile normalized. All spot replicates were pooled using the avereps function, producing an Elist containing $\log_2$ relative expression data. Values of the negative control spots were subtracted from the mean intensities and all negative probes were removed. Expression values were calculated as mean values of the dipteran miRNA expression of the four biological replicates. As the microarray contained miRNAs of multiple insect species including miRNA orthologs, only probes with at least 14 nucleotides complementary to the annotated *A. gambiae* miRNAs were included in further analysis. In total, 506 microarray probes were included, representing 86 mature *A. gambiae* miRNAs annotated in the miRBase (Supplemental Material, Table S1 in File S1). Differentially regulated miRNAs were identified by fitting a linear regression model to the data and empirical Bayes statistics on the model in R. All microarray probes that differ in sequence were analyzed and visualized separately. Finally, we aimed to provide an overview of miRNA enrichment in mosquito tissues. To this end, we set an enrichment cut-off of 1.5-fold (Figure 6). Two studies in *A. gambiae* and *Ae. aegypti* showed that miR-1175-3p is a midgut-specific miRNA (Winter *et al.* 2007; Liu *et al.* 2014). We gauged expression levels of this miRNA across different tissues and observed a 1.5-fold higher expression of miR-1175 in the midgut compared to other tissues. Therefore, we applied this cut-off to other miRNAs.

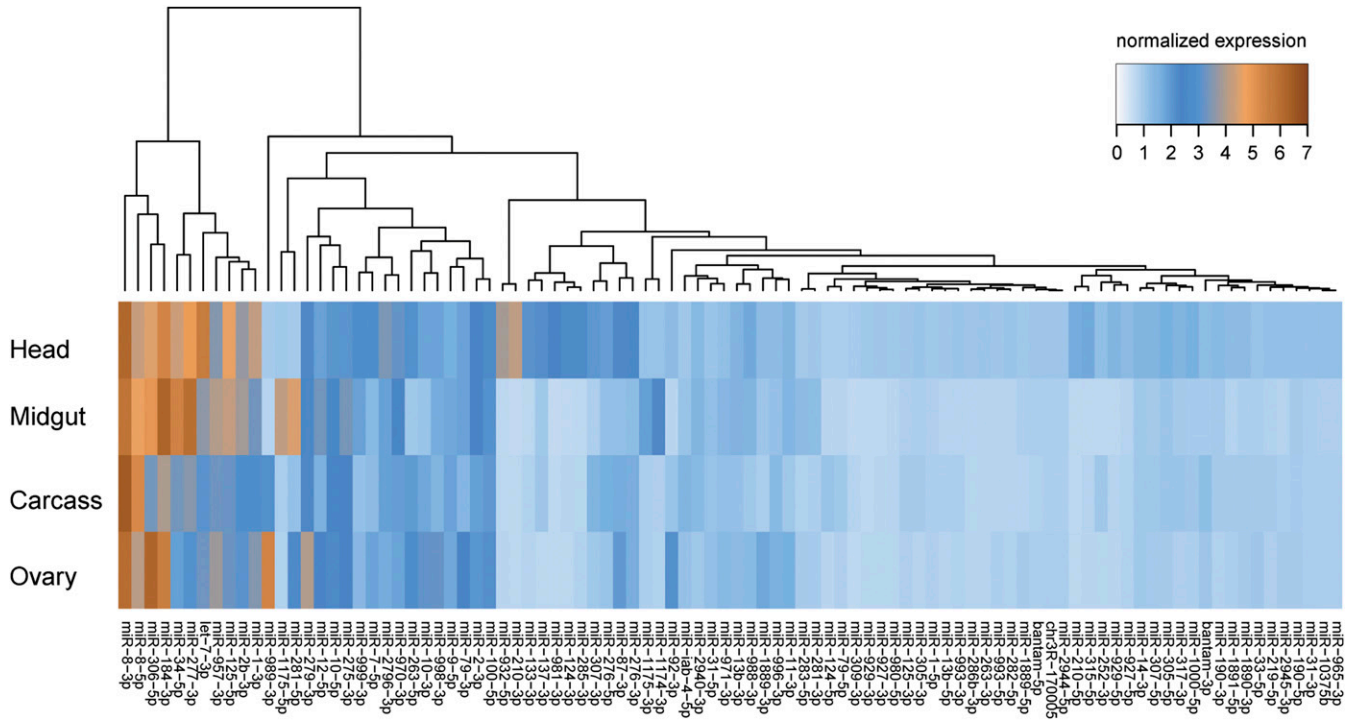

Figure 2 Tissue-specific microRNA (miRNA) expression in the 3-d-old *A. gambiae* female. Heatmap of miRNA expression levels in the head, midgut, fat body, and ovaries of sugar-fed mosquitoes in the previtellogenic phase. Color gradient from light blue to dark brown represents an increase in miRNA expression.

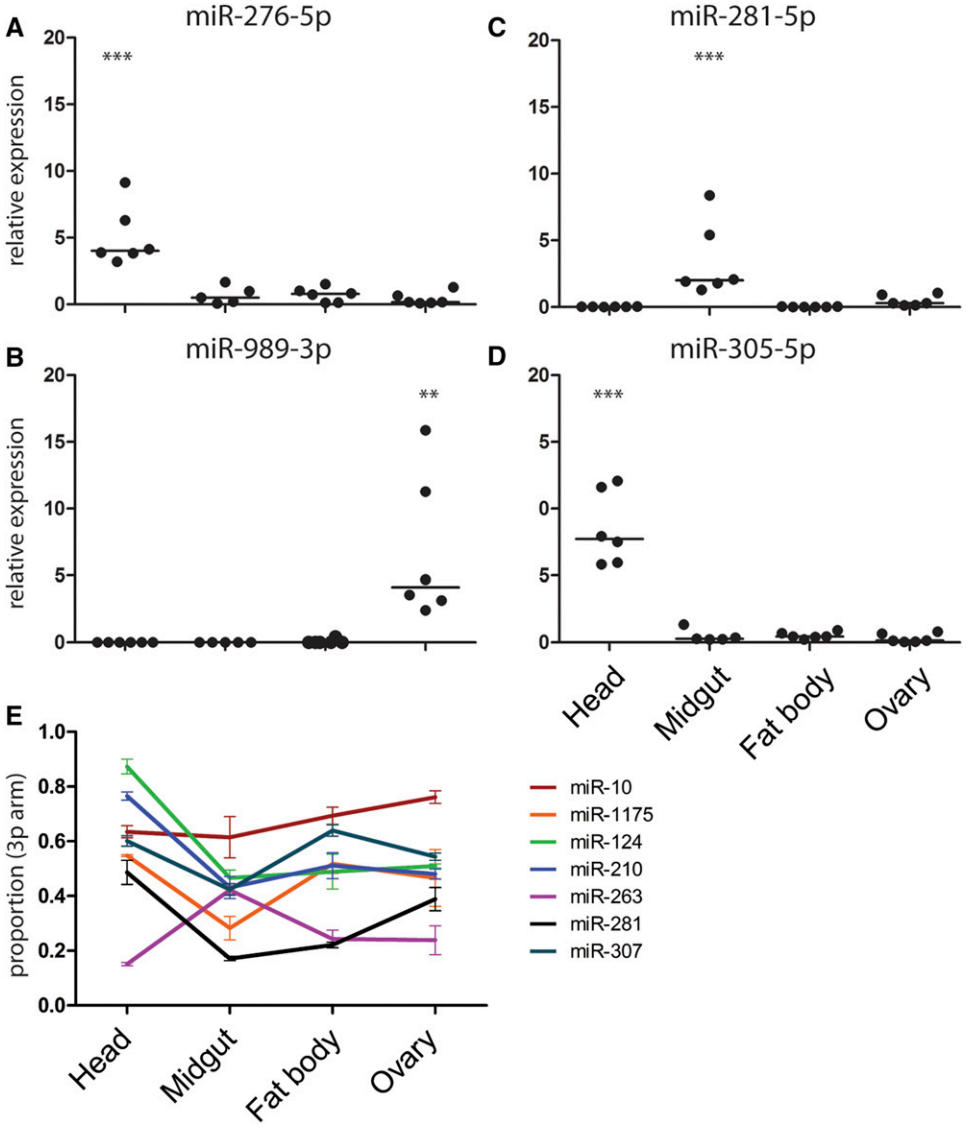

Figure 3 Tissue-specific expression of microRNAs (miRNAs) quantified by quantitative polymerase chain reaction of (A) miR-276-5p, (B) miR-281-5p, (C) miR-989-3p, and (D) miR-305-5p. miRNA expression values are plotted as dots with the line indicating the mean. miRNA expression levels were normalized using the ribosomal protein RPS7 gene. Results of six independent experiments are shown. ** $P < 0.005$ and *** $P < 0.0005$, one-way ANOVA followed by Tukey's *post hoc* test. (E) Tissue-specific differences in miRNA 3p-arm proportion. All depicted 3p-arm proportions significantly change between tissues tested by one-way ANOVA (*P*-value < 0.05; Table S3 in File S1).

cDNA synthesis and qPCR

Total RNA was reverse-transcribed with the miScript Kit (QIAGEN). Expression levels of mature miRNAs and of mRNAs were measured using the Quantitect SYBR Green PCR Kit (QIAGEN). Relative quantities of miRNA expression were normalized to the gene encoding ribosomal protein S7 (*RPS7*). The miRNA primers were obtained as miRNA Primer Assays (QIAGEN).

Data availability

Mosquito and parasite strains are available on request. The code for microarray analysis was written in R and is available on GitHub in the repository LenaLampe/Microarray-Analysis (https://github.com/LenaLampe/Microarray-Analysis). The raw data files are available at the Gene Expression Omnibus (GSE103034). Table S4 in File S1 contains a description of the files.

RESULTS

We set out to develop a global overview of tissue-specific miRNA expression in the head, midgut, ovary, and fat body, during the gonotrophic cycle of *A. gambiae* and after *P. falciparum* infections. To this end, we determined miRNA expression levels using the Agilent custom-designed miRNA microarray in the three groups of females fed with: (1) sugar; (2) human blood, or (3) *P. falciparum*-infected blood (Figure 1).

MicroRNA expression in the PV phase

We first examined expression levels of miRNAs in the PV phase. Microarray analysis detected expression of 74 out of 86 miRNAs in at least one tissue. The microarray probes matched almost all *A. gambiae* miRNAs annotated in the miRBase, as well as the highly conserved insect miRNAs (Table S1 in File S1). One limitation of the microarray approach is that it is applicable only to known miRNAs. Instead, RNA-seq technologies are better suited for discovery of novel miRNAs and for overcoming problems of cross-kingdom miRNA hybridization in blood-fed mosquitoes. The problem of RNA-seq is its quantitative inaccuracy, as the majority of the newly identified *Anopheles*-specific miRNAs reported by previous studies are expressed at very low levels (Biryukova *et al.* 2014; Castellano *et al.* 2015). Therefore, our microarray approach covers the more highly expressed, as well as conserved, miRNAs. High levels of expression across all tissues were detected only for miR-8, whereas nine miRNAs (miR-1, miR-2, let-7, miR-34,

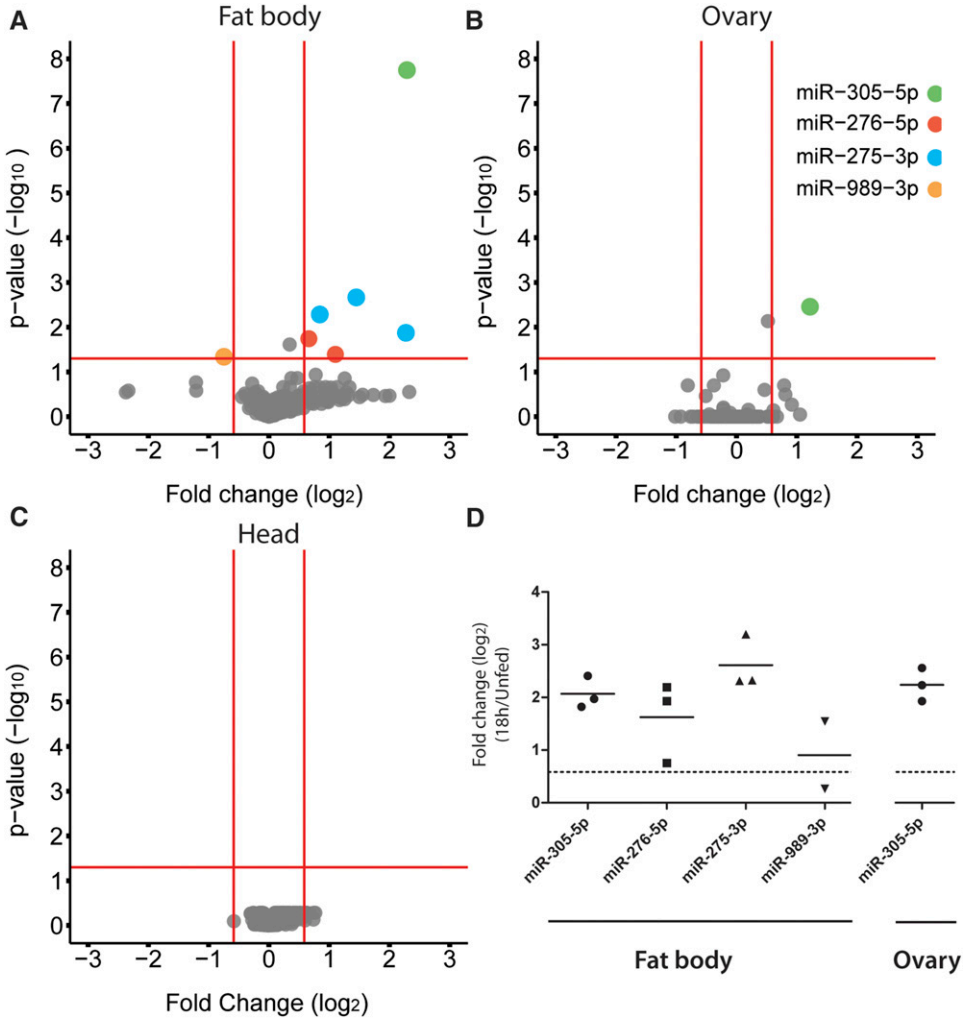

Figure 4 Differentially expressed microRNAs (miRNAs) at 18 hr post-feeding (hpb) in: (A) the fat body, (B) the ovaries, and (C) the head. Cut-off $\log_{10}$ *P*-value of ± 1.3 ($P < 0.05$) and $\log_2$ fold change of ± 0.58 (FC > 1.5) ($n = 4$) were used to detect significant changes in miRNA expression by fitting a linear model with empirical Bayes statistics. The dots represent different miRNA probes. (D) Blood feeding-induced changes ($\log_2$ FC) in the fat body and ovary of miRNA expression levels at 18 hpb measured by quantitative polymerase chain reaction. Results of three independent experiments are shown, horizontal lines indicate mean values.

miR-125, miR-184, miR-277, miR-306, and miR-957) had moderate to high levels of expression in at least two tissues (Figure 2). A second cluster of 18 miRNAs included tissue-specific miRNAs with intermediate expression levels. The largest number of tissue-specific miRNAs (cut-off 1.5-fold) was observed in the head (17 miRNAs), including the well-known brain-enriched miR-7 and miR-124. Three miRNAs—miR-281, miR-1174, and miR-1175—were enriched in the midgut, whereas miR-10, miR-92b, miR-279, miR-989, and miR-998 were predominantly detected in the ovaries. Surprisingly, not a single miRNA was exclusively expressed in the fat body. Microarray results were further validated by independent quantitative PCR (Figure 3, A–D).

The mature miRNA can be generated from the 3p or 5p arm of the pre-miRNA. We used arm-specific probes to quantify tissue-specific expression of miRNA arms and identified 20 miRNAs expressing both arms (Table S2 in File S1). Among those, seven miRNAs showed tissue-dependent arm bias (Figure 3E, Table S3 in File S1). Head-specific enrichment in the 3p arm was observed for miR-124 and miR-210, whereas the 5p arm bias was detected for miR-1175 in the midgut and for miR-263 in the head, fat body, and ovaries. Furthermore, higher levels of the 5p arm were detected in the head and midgut for miR-10. A complex pattern of arm usage was observed for miR-281 and miR-307. While the miR-281-5p was enriched in the fat body and midgut, expression of the 3p arm increased in the head and ovary. For miR-307, the 3p arm was predominantly expressed in the head and fat body. We concluded that, during the PV phase, expression of the majority of the miRNAs is tissue-specific and, in some cases, is regulated at the arm level.

Tissue-specific miRNA expression after blood feeding and after P. falciparum infection

We next examined miRNA expression during the PBM phase and after *P. falciparum* infection at 18 hpb (Figure S1). At this time point, all midgut samples from blood-fed females had high background levels, probably due to unspecific binding of human short RNAs and DNAs present in the blood meal. Therefore, we excluded these samples from further analyses. Interestingly, blood feeding impacted expression levels of very few miRNAs in other tissues. Major changes were observed in the fat body, where blood feeding increased levels of miR-275-3p, miR-276-5p, and miR-305-5p, and reduced levels of miR-989-3p (Figure 4A). Higher levels of miR-305-5p were also detected in the ovaries (Figure 4B). No changes in miRNA levels after blood meal were observed in the head (Figure 4C). Surprisingly, infections with *P. falciparum* had no effect on miRNA expression in any tested tissue (Figure S2, A–C). The expression changes detected by microarray analysis were further confirmed by qPCR, except for miR-989-3p with very low expression levels in the fat body (Figure 4D). Taken together, our results identified three miRNAs whose expression was modulated during the PV to PBM

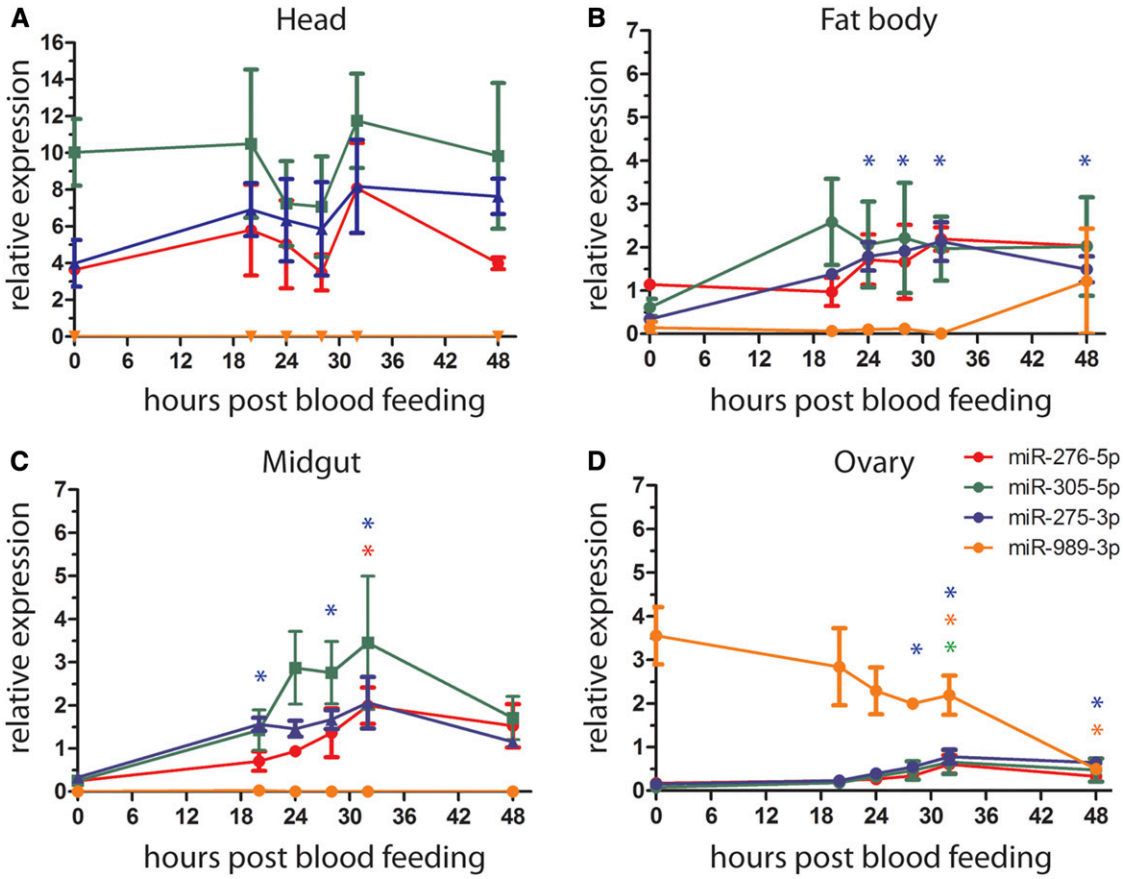

Figure 5 Tissue-specific expression of miR-276-5p, miR-305-5p, miR-275-3p, and miR-989-3p during the postblood meal phase in (A) the head, (B) the fat body, (C) the midgut, and (D) the ovary. Results of three independent experiments are shown as mean ± SEM. For statistical analyses, all time points were compared to 0 hr (unfed) by one-way ANOVA, Tukey's *post hoc* test and significant differences are shown by asterisk (* $P < 0.05$; $n = 5$).

transition in the fat body, whereas expression of miR-305-5p was also upregulated in the ovaries.

Expression of blood meal-induced miRNAs during the PBM phase

The kinetics of tissue-specific expression of the blood feeding-induced miRNAs was further analyzed by qPCR. The highest expression levels of miR-305-5p, miR-275-3p, and miR-276-5p were observed in the head before blood feeding, while expression of miR-989-3p was only detected in the ovaries (Figure 5A). Expression levels of miR-275-3p, miR-276-5p, and miR-305-5p transiently declined in the head at 24 and 28 hpb, and regained the initial levels by 32 hpb (Figure 5A). In contrast, high levels of these miRNAs were detected in the fat body and midgut at the same time points (Figure 5, B and C). In the fat body, miR-275-3p and miR-276-5p levels peaked at 28 and 32 hpb, and remained high at 48 hpb. High interreplicate variation was observed for miR-305-5p, whose levels increased between 20 and 48 hpb (Figure 5B). In the midgut, miR-275-3p, miR-276-5p, and miR-305-5p peaked at 24–32 hpb, but, in contrast to the fat body, their levels slightly declined by 48 hr PBM (Figure 5C). High expression levels of miR-989-3p detected in the ovaries before blood feeding gradually declined during 48 hpb. In contrast, low transcript levels of miR-305-5p, miR-275-3p, and miRNA-276-5p in the ovaries slightly increased at 28 and 32 hpb (Figure 5D). We concluded that PV to PBM transition regulates miRNA expression levels in a tissue- and time-specific manner.

DISCUSSION

We report a global overview of miRNA expression in the *A. gambiae* tissues during the late PV and PBM phases. We found that the majority of *A. gambiae* miRNAs are expressed in a tissue-specific manner, with the exception of the ubiquitously highly expressed miR-8. While six miRNAs showed tissue-specific bias in arm expression, one-third of the miRNAs expressed both arms. Previous RNA sequencing studies of whole mosquitoes identified miR-10, miR-184, miR-263, miR-281, and miR-306 as the most abundant miRNAs in adult females (Biryukova *et al.* 2014; Castellano *et al.* 2015). We show that expression of these abundant miRNAs is restricted to specific tissues (Figure 6A). These results are in agreement with functional specialization of tissues, which is in part regulated by miRNAs (Jin *et al.* 2012; Loya *et al.* 2014; Lee *et al.* 2015).

Reproduction in many mosquito species is tightly coupled to blood feeding. During the PV phase, females feed on sugars to increase energy reserves for efficient egg development (Hou *et al.* 2015; Wang *et al.* 2017). Previous reports have shown that miR-1174 regulates sugar absorption in the midgut of *Aedes* female mosquitoes (Liu *et al.* 2014). We demonstrate conservation of the midgut-specific expression of miR-1174/1175 and miR-281 between *A. gambiae* and *Ae. aegypti* (Winter *et al.* 2007; Liu *et al.* 2014; Zhou *et al.* 2014). In addition, we also observed high levels of miR-277 in the midgut. *Drosophila* miR-277 regulates branched-chain amino acid (BCAA) catabolism and activates TOR signaling in the thoracic muscles (Esslinger *et al.* 2013).

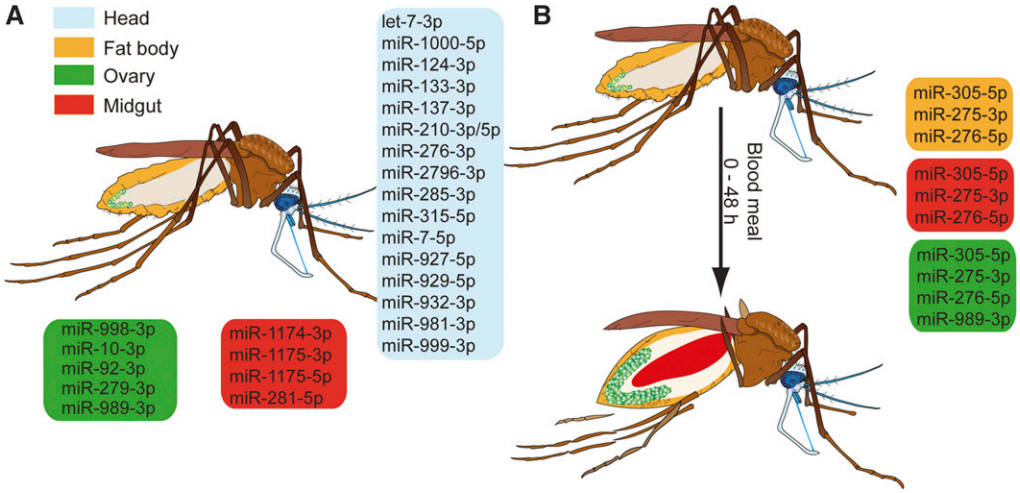

Figure 6 Schematic summary of tissue-specific microRNA (miRNA) expression during the gonotrophic cycle of the female *A. gambiae* mosquito (A) Tissue-enriched miRNAs in sugar-fed mosquitoes. Enrichment cut-off for tissue-specific miRNAs was set at 1.5-fold. (B) miRNAs regulated during the postblood meal phase. The colored boxes show tissue-specific miRNAs (blue = head, yellow = fat body, green = ovary, and red = midgut).

BCAAs serve as signaling metabolites in tissue communication, systemically promote anabolic metabolism, and release hormones from the intestinal tract in mice (Nishitani *et al.* 2002; Ijichi *et al.* 2003; She *et al.* 2007; Chen and Reimer 2009). It is possible, that BCAA catabolism in the midgut signals food uptake to distant tissues. Further investigations of miR-277 function in the midgut are needed to explore an interesting link between food digestion, TOR signaling, and systemic metabolic changes. TOR signaling is tightly connected to synthesis of JH, the major driver of the PV phase (Pérez-Hedo *et al.* 2013). During insect development, systemic JH levels serve as a checkpoint for sufficient energy reserves and body size before transition to the next developmental stage. *Drosophila* miR-2 generates a threshold for developmental transitions by regulating downstream JH signaling (Lozano *et al.* 2015). The rise of JH levels with nutrient availability during the PV phase suggests that the JH checkpoint's function may also be conserved in mosquitoes (Shiao *et al.* 2008; Clifton and Noriega 2011; Perez-Hedo *et al.* 2014). Furthermore, high expression levels of miR-2 in the PV phase indicate that expression of this miRNA may also regulate JH signaling in *A. gambiae*.

Brain tissues, especially the central nervous system, play essential roles in the PV phase by regulating mosquito olfactory and circadian behaviors (Carey *et al.* 2010; Kessler *et al.* 2015). Efficient response to blood feeding depends on timely accumulation of the ovary ecdysteroidogenic hormone in the granules of neurosecretory cells (Brown and Cao 2001). We found that the majority of the tissue-specific miRNAs are expressed in the head, including the well-known miRNAs that regulate olfactory sensing and circadian rhythms (Li *et al.* 2013; Wang *et al.* 2014; Chen and Rosbash 2016; Garaulet *et al.* 2016; Zhang *et al.* 2016a). In mosquitoes, these processes shape such important vector competence traits as host seeking and biting behavior; therefore, further investigation of the head-specific miRNAs should identify new factors and mechanisms that regulate vector competence.

Although feeding induces massive physiological changes in the mosquito, we identified only modest changes in expression levels of miRNAs during the early PBM phase in the head, fat body, and ovaries (Figure 6B). Note that no information could be generated for the midgut tissues pending the technical problem of cross-hybridization. Interestingly, blood meal-induced miRNAs in the fat body follow similar expression patterns in the midgut, indicating potential roles of these miRNAs in the regulation of mosquito metabolism. In line with this hypothesis, miR-275 and miR-305 modulate metabolic processes in other insects. In *Ae. aegypti*, miR-275 ensures successful blood meal digestion, fluid excretion, and, consequently, egg development (Bryant *et al.* 2010). In agreement with miR-275 expression patterns in *A. gambiae*, TOR and ecdysone control expression of this miRNA in *Ae. aegypti* (Bryant *et al.* 2010). Similarly, TOR and insulin pathways in *Drosophila* regulate expression of miR-305 in the fat body and the gut, respectively, where miR-305 fosters adaptation to starvation by balancing stem cell renewal and differentiation in a nutrient-dependent context (Barrio *et al.* 2014; Foronda *et al.* 2014). Interestingly, increased levels of miR-305 in the midgut 24 hr after *P. falciparum* infection negatively impact parasite development in *A. gambiae* (Dennison *et al.* 2015). Although the mechanisms of parasite inhibition are currently unknown, it is plausible that miR-305 affects *Plasmodium* development by regulating midgut homeostasis and/or nutrient availability. Further studies should examine whether the effect of miR-305 on *Plasmodium* development is midgut-specific. We did not detect any miRNAs regulated by *P. falciparum* infection in the head, fat body, and ovaries during the early PBM phase. Whether parasite replication regulates miRNA expression during later stages of the PBM phase remains to be investigated.

As ovary growth and maturation is initiated in the second half of the PBM phase, it is not surprising that we detected only minor changes in the expression levels of ovarian miRNAs. Indeed, at 24 hr PBM, the oocytes only begin to accumulate lipids necessary for their maturation. Nevertheless, the observed downregulation of miR-989 coincides in time with the initiation of border cell migration, which in *Drosophila* is regulated by miR-989 (Kugler *et al.* 2013). Therefore, *A. gambaie* miR-989 may have a conserved role in the induction of oogenesis.

Collectively, our results show tissue-specific expression patterns of 74 *A. gambiae* miRNAs during the PV and PBM phases. Recent metabolic studies during the gonotrophic cycle in *Aedes* mosquitoes have identified the highest metabolic activity at 36 hpb in the fat body (Hou *et al.* 2015; Wang *et al.* 2017). Therefore, we propose that the tissue-specific modulation of miRNA expression by blood feeding reported in this study may contribute to the regulation of metabolic changes during the mosquito gonotrophic cycle.

ACKNOWLEDGMENTS

We thank Liane Spohr and Sandrina Koppitz for mosquito breeding, as well as Dana Tschierske and Daniel Eyermann for cultivation of the *P. falciparum* parasite. We thank Hilary Ranson, Craig Wilding, and

Inna Biryukova for sharing the custom microarray design, and we acknowledge the technical support of Hans-Joachim Mollenkopf and Ina Wagner from the microarray core facility at the Max Planck Institute for Infection Biology. We are also grateful to Maiara Severo for comments on the manuscript. L.L. acknowledges support by the Center of Infection and Immunity (ZIBI) and the ZIBI Graduate School.

LITERATURE CITED

Atella, G. C., P. R. Bittencourt-Cunha, R. D. Nunes, M. Shahabuddin, and M. A. C. Silva-Neto, 2009 The major insect lipoprotein is a lipid source to mosquito stages of malaria parasite. Acta Trop. 109: 159–162.

Attardo, G. M., I. A. Hansen, and A. S. Raikhel, 2005 Nutritional regulation of vitellogenesis in mosquitoes: implications for anautogeny. Insect Biochem. Mol. Biol. 35: 661–675.

Barrio, L., A. Dekanty, and M. Milán, 2014 MicroRNA-mediated regulation of Dp53 in the *Drosophila* fat body contributes to metabolic adaptation to nutrient deprivation. Cell Rep. 8: 528–541.

Beier, J. C., 1998 Malaria parasite development in mosquitoes. Annu. Rev. Entomol. 43: 519–543.

Bennink, S., M. J. Kiesow, and G. Pradel, 2016 The development of malaria parasites in the mosquito midgut. Cell. Microbiol. 18: 905–918.

Biryukova, I., T. Ye, E. Levashina, N. Pakpour, V. Corby-Harris *et al.*, 2014 Transcriptome-wide analysis of microRNA expression in the malaria mosquito *Anopheles gambiae*. BMC Genomics 15: 557.

Boulan, L., D. Martín, and M. Milán, 2013 Bantam miRNA promotes systemic growth by connecting insulin signaling and ecdysone production. Curr. Biol. 23: 473–478.

Brown, M. R., and C. Cao, 2001 Distribution of ovary ecdysteroidogenic hormone I in the nervous system and gut of mosquitoes. J. Insect Sci. 1: 3.

Bryant, B., W. Macdonald, and A. S. Raikhel, 2010 microRNA miR-275 is indispensable for blood digestion and egg development in the mosquito *Aedes aegypti*. Proc. Natl. Acad. Sci. USA 107: 22391–22398.

Carey, A. F., G. Wang, C.-Y. Su, L. J. Zwiebel, and J. R. Carlson, 2010 Odorant reception in the malaria mosquito *Anopheles gambiae*. Nature 464: 66–71.

Castellano, L., E. Rizzi, J. Krell, M. Di Cristina, R. Galizi *et al.*, 2015 The germline of the malaria mosquito produces abundant miRNAs, endo-siRNAs, piRNAs and 29-nt small RNAs. BMC Genomics 16: 100.

Chen, Q., and R. A. Reimer, 2009 Dairy protein and leucine alter GLP-1 release and mRNA of genes involved in intestinal lipid metabolism in vitro. Nutrition 25: 340–349.

Chen, X., and M. Rosbash, 2016 mir-276a strengthens *Drosophila* circadian rhythms by regulating timeless expression. Proc. Natl. Acad. Sci. USA 113: E2965–E2972.

Chiang, H. R., L. W. Schoenfeld, J. G. Ruby, V. C. Auyeung, N. Spies *et al.*, 2010 Mammalian microRNAs: experimental evaluation of novel and previously annotated genes. Genes Dev. 24: 992–1009.

Childs, L. M., F. Y. Cai, E. G. Kakani, S. N. Mitchell, D. Paton *et al.*, 2016 Disrupting mosquito reproduction and parasite development for malaria control. PLoS Pathog. 12: e1006060.

Clifton, M. E., and F. G. Noriega, 2011 Nutrient limitation results in juvenile hormone-mediated resorption of previtellogenic ovarian follicles in mosquitoes. J. Insect Physiol. 57: 1274–1281.

Costa, G., M. Eldering, R. L. Lindquist, A. E. Hauser, R. Sauerwein *et al.*, 2017 Non-competitive resource exploitation within-mosquito shapes evolution of malaria virulence bioRxiv DOI: 10.1101/149443.

Dennison, N. J., O. J. BenMarzouk-Hidalgo, and G. Dimopoulos, 2015 MicroRNA-regulation of *Anopheles gambiae* immunity to *Plasmodium falciparum* infection and midgut microbiota. Dev. Comp. Immunol. 49: 170–178.

Esslinger, S. M., B. Schwalb, S. Helfer, K. M. Michalik, H. Witte *et al.*, 2013 *Drosophila* miR-277 controls branched-chain amino acid catabolism and affects lifespan. RNA Biol. 10: 1042–1056.

Foronda, D., R. Weng, P. Verma, Y.-W. Chen, and S. M. Cohen, 2014 Coordination of insulin and Notch pathway activities by microRNA miR-305 mediates adaptive homeostasis in the intestinal stem cells of the *Drosophila* gut. Genes Dev. 28: 2421–2431.

Fu, X., G. Dimopoulos, and J. Zhu, 2017 Association of microRNAs with Argonaute proteins in the malaria mosquito *Anopheles gambiae* after blood ingestion. Sci. Rep. 7: 6493.

Garaulet, D. L., K. Sun, W. Li, J. Wen, A. M. Panzarino *et al.*, 2016 miR-124 regulates diverse aspects of rhythmic behavior in *Drosophila*. J. Neurosci. 36: 3414–3421.

Hagedorn, H. H., J. D. O'Connor, M. S. Fuchs, B. Sage, D. A. Schlaeger *et al.*, 1975 The ovary as a source of alpha-ecdysone in an adult mosquito. Proc. Natl. Acad. Sci. USA 72: 3255–3259.

Hagedorn, H. H., S. Turner, E. A. Hagedorn, D. Pontecorvo, P. Greenbaum *et al.*, 1977 Postemergence growth of the ovarian follicles of *Aedes aegypti*. J. Insect Physiol. 23: 203–206.

Hansen, I. A., G. M. Attardo, J.-H. Park, Q. Peng, and A. S. Raikhel, 2004 Target of rapamycin-mediated amino acid signaling in mosquito anautogeny. Proc. Natl. Acad. Sci. USA 101: 10626–10631.

Hansen, I. A., G. M. Attardo, S. G. Roy, and A. S. Raikhel, 2005 Target of rapamycin-dependent activation of S6 kinase is a central step in the transduction of nutritional signals during egg development in a mosquito. J. Biol. Chem. 280: 20565–20572.

Hansen, I. A., G. M. Attardo, S. D. Rodriguez, and L. L. Drake, 2014 Four-way regulation of mosquito yolk protein precursor genes by juvenile hormone-, ecdysone-, nutrient-, and insulin-like peptide signaling pathways. Front. Physiol. 5: 103.

Hou, Y., X.-L. Wang, T. T. Saha, S. Roy, B. Zhao *et al.*, 2015 Temporal coordination of carbohydrate metabolism during mosquito reproduction. PLoS Genet. 11: e1005309.

Ijichi, C., T. Matsumura, T. Tsuji, and Y. Eto, 2003 Branched-chain amino acids promote albumin synthesis in rat primary hepatocytes through the mTOR signal transduction system. Biochem. Biophys. Res. Commun. 303: 59–64.

Jin, H., V. N. Kim, and S. Hyun, 2012 Conserved microRNA miR-8 controls body size in response to steroid signaling in *Drosophila*. Genes Dev. 26: 1427–1432.

Kessler, S., M. Vlimant, and P. M. Guerin, 2015 Sugar-sensitive neurone responses and sugar feeding preferences influence lifespan and biting behaviours of the Afrotropical malaria mosquito, *Anopheles gambiae*. J. Comp. Physiol. A Neuroethol. Sens. Neural Behav. Physiol. 201: 317–329.

Kugler, J.-M., Y.-W. Chen, R. Weng, S. M. Cohen, D. Bartel *et al.*, 2013 miR-989 is required for border cell migration in the *Drosophila* ovary. PLoS One 8: 215–233.

Lee, G. J., J. W. Jun, and S. Hyun, 2015 MicroRNA miR-8 regulates multiple growth factor hormones produced from *Drosophila* fat cells. Insect Mol. Biol. 24: 311–318.

Lensen, A., J. van Druten, M. Bolmer, G. van Gemert, W. Eling *et al.*, 1996 Measurement by membrane feeding of reduction in *Plasmodium falciparum* transmission induced by endemic sera. Trans. R. Soc. Trop. Med. Hyg. 90: 20–22.

Lensen, A., A. Bril, M. Van de Vegte, G. J. van Gemert, W. Eling *et al.*, 1999 Infectivity of cultured *Plasmodium falciparum* gametocytes to mosquitoes. Exp. Parasitol. 91: 101–103.

Li, W., M. Cressy, H. Qin, T. Fulga, D. Van Vactor *et al.*, 2013 MicroRNA-276a functions in ellipsoid body and mushroom body neurons for naive and conditioned olfactory avoidance in *Drosophila*. J. Neurosci. 33: 5821–5833.

Liu, S., K. J. Lucas, S. Roy, J. Ha, and A. S. Raikhel, 2014 Mosquito-specific microRNA-1174 targets serine hydroxymethyltransferase to control key functions in the gut. Proc. Natl. Acad. Sci. USA 111: 14460–14465.

Loya, C. M., E. M. McNeill, H. Bao, B. Zhang, and D. Van Vactor, 2014 miR-8 controls synapse structure by repression of the actin regulator enabled. Development 141: 1864–1874.

Lozano, J., R. Montañez, and X. Belles, 2015 MiR-2 family regulates insect metamorphosis by controlling the juvenile hormone signaling pathway. Proc. Natl. Acad. Sci. USA 112: 3740–3745.

Lu, T., Y. T. Qiu, G. Wang, J. Y. Kwon, M. Rutzler *et al.*, 2007 Odor coding in the maxillary palp of the malaria vector mosquito *Anopheles gambiae*. Curr. Biol. 17: 1533–1544.

Lucas, K. J., S. Roy, J. Ha, A. L. Gervaise, V. A. Kokoza *et al.*, 2015a MicroRNA-8 targets the Wingless signaling pathway in the female mosquito fat body to regulate reproductive processes. Proc. Natl. Acad. Sci. USA 112: 1440–1445.

Lucas, K. J., B. Zhao, S. Roy, A. L. Gervaise, and A. S. Raikhel, 2015b Mosquito-specific microRNA-1890 targets the juvenile hormone-regulated serine protease JHA15 in the female mosquito gut. RNA Biol. 12: 1383–1390.

Marco, A., J. H. L. Hui, M. Ronshaugen, and S. Griffiths-Jones, 2010 Functional shifts in insect microRNA evolution. Genome Biol. Evol. 2: 686–696.

Nishitani, S., T. Matsumura, S. Fujitani, I. Sonaka, Y. Miura *et al.*, 2002 Leucine promotes glucose uptake in skeletal muscles of rats. Biochem. Biophys. Res. Commun. 299: 693–696.

Park, J.-H., G. M. Attardo, I. A. Hansen, and A. S. Raikhel, 2006 GATA factor translation is the final downstream step in the amino acid/target-of-rapamycin-mediated vitellogenin gene expression in the anautogenous mosquito *Aedes aegypti*. J. Biol. Chem. 281: 11167–11176.

Pérez-Hedo, M., C. Rivera-Perez, and F. G. Noriega, 2013 The insulin/TOR signal transduction pathway is involved in the nutritional regulation of juvenile hormone synthesis in *Aedes aegypti*. Insect Biochem. Mol. Biol. 43: 495–500.

Perez-Hedo, M., C. Rivera-Perez, and F. G. Noriega, 2014 Starvation increases insulin sensitivity and reduces juvenile hormone synthesis in mosquitoes. PLoS One 9: e86183.

Rono, M. K., M. M. A. Whitten, M. Oulad-Abdelghani, E. A. Levashina, and E. Marois, 2010 The major yolk protein vitellogenin interferes with the anti-*Plasmodium* response in the malaria mosquito *Anopheles gambiae*. PLoS Biol. 8: e1000434.

Shapiro, J. P., and H. H. Hagedorn, 1982 Juvenile hormone and the development of ovarian responsiveness to a brain hormone in the mosquito, *Aedes aegypti*. Gen. Comp. Endocrinol. 46: 176–183.

She, P., T. M. Reid, S. K. Bronson, T. C. Vary, A. Hajnal *et al.*, 2007 Disruption of BCATm in mice leads to increased energy expenditure associated with the activation of a futile protein turnover cycle. Cell Metab. 6: 181–194.

Shiao, S.-H., I. A. Hansen, J. Zhu, D. H. Sieglaff, and A. S. Raikhel, 2008 Juvenile hormone connects larval nutrition with target of rapamycin signaling in the mosquito *Aedes aegypti*. J. Insect Physiol. 54: 231–239.

Smykal, V., and A. S. Raikhel, 2015 Nutritional control of insect reproduction. Curr. Opin. Insect Sci. 11: 31–38.

Spielman, A., R. W. Gwadz, and W. A. Anderson, 1971 Ecdysone-initiated ovarian development in mosquitoes. J. Insect Physiol. 17: 1807–1814.

Verma, P., and S. M. Cohen, 2015 miR-965 controls cell proliferation and migration during tissue morphogenesis in the *Drosophila* abdomen. Elife 4: 1–18.

Wang, C., T. Feng, Q. Wan, Y. Kong, and L. Yuan, 2014 miR-124 controls *Drosophila* behavior and is required for neural development. Int. J. Dev. Neurosci. 38: 105–112.

Wang, X., Y. Hou, T. T. Saha, G. Pei, A. S. Raikhel *et al.*, 2017 Hormone and receptor interplay in the regulation of mosquito lipid metabolism. Proc. Natl. Acad. Sci. USA 114: E2709–E2718.

Winter, F., S. Edaye, A. Hüttenhofer, and C. Brunel, 2007 *Anopheles gambiae* miRNAs as actors of defence reaction against *Plasmodium* invasion. Nucleic Acids Res. 35: 6953–6962.

Zhang, Y., P. Lamba, P. Guo, and P. Emery, 2016a miR-124 regulates the phase of *Drosophila* circadian locomotor behavior. J. Neurosci. 36: 2007–2013.

Zhang, Y., B. Zhao, S. Roy, T. T. Saha, V. A. Kokoza *et al.*, 2016b microRNA-309 targets the Homeobox gene SIX4 and controls ovarian development in the mosquito *Aedes aegypti*. Proc. Natl. Acad. Sci. USA 113: E4828–E4836.

Zhou, H., M. L. Arcila, Z. Li, E. J. Lee, C. Henzler *et al.*, 2012 Deep annotation of mouse iso-miR and iso-moR variation. Nucleic Acids Res. 40: 5864–5875.

Zhou, Y., Y. Liu, H. Yan, Y. Li, H. Zhang *et al.*, 2014 miR-281, an abundant midgut-specific miRNA of the vector mosquito *Aedes albopictus* enhances dengue virus replication. Parasit. Vectors 7: 488.

Zhu, J., L. Chen, G. Sun, and A. S. Raikhel, 2006 The competence factor beta Ftz-F1 potentiates ecdysone receptor activity via recruiting a p160/SRC coactivator. Mol. Cell. Biol. 26: 9402–9412.

Communicating editor: M. Boutros